

Research

A novel M2-like tumor associated macrophages-related gene signature for predicting the prognosis and immunotherapy efficacy in gastric cancer

Xuezh Li¹ · Xiaodong Qu¹ · Na Wang¹ · Songbo Li¹ · Xingyu Zhao¹ · Kexin Lin¹ · Yongquan Shi¹

Received: 16 February 2024 / Accepted: 5 August 2024

Published online: 16 August 2024

© The Author(s) 2024 [OPEN](#)

Abstract

Background M2-like tumor-associated macrophages (M2-like TAMs) play key roles in tumor progression and the immune response. However, the clinical significance and prognostic value of M2-like TAMs-associated regulatory genes in gastric cancer (GC) have not been clarified.

Methods Herein, we identified M2-like TAM-related genes by weighted gene coexpression network analysis of TCGA-STAD and GSE84437 cohort. Lasso-Cox regression analyses were then performed to screen for signature genes, and a novel signature was constructed to quantify the risk score for each patient. Tumor mutation burden (TMB), survival outcomes, immune cells, and immune function were analyzed in the risk groups to further reveal the immune status of GC patients. A gene-drug correlation analysis and sensitivity analysis of anticancer drugs were used to identify potential therapeutic agents. Finally, we verified the mRNA expression of signature genes in patient tissues by qRT-PCR, and analyzed the expression distribution of these genes by IHC.

Results A 4-gene (SERPINE1, MATN3, CD36, and CNTN1) signature was developed and validated, and the risk score was shown to be an independent prognostic factor for GC patients. Further analyses revealed that GC patients in the high-risk group had a worse prognosis than those in the low-risk group, with significant differences in TMB, clinical features, enriched pathways, TIDE score, and tumor microenvironment features. Finally, we used qRT-PCR and IHC analysis to verify mRNA and protein level expression of signature genes.

Conclusion These findings highlight the importance of M2-like TAMs, provide a new perspective on individualized immunotherapy for GC patients.

Keywords Gastric cancer · M2-like TAMs · Signature · Immune landscape · Immunotherapy response

Xuezh Li and Xiaodong Qu contributed equally to this work.

Supplementary Information The online version contains supplementary material available at <https://doi.org/10.1007/s12672-024-01221-8>.

✉ Yongquan Shi, shiyquan@fmmu.edu.cn | ¹State key Laboratory of Cancer Biology and National Clinical Research Center for Digestive Diseases, Xijing Hospital of Digestive Diseases, Fourth Military Medical University, Xi'an, China.



1 Introduction

Gastric cancer (GC) remains a highly prevalent and fatal malignancy with high prevalence and mortality rate. A total of 1.08 million patients are diagnosed with GC each year, with more than 770,000 deaths [1]. Although the level of clinical diagnosis has improved and chemotherapy regimens have been enriched in recent years, the survival rate of gastric cancer patients is still relatively low [2]. The pathogenesis of GC has not yet been elucidated, and there is a lack of effective means of treatment, resulting in an unpromising prognosis [3]. Therefore, the construction of new clinical predictive signature and the study of gene expression related to GC are expected to understand the development of GC at the molecular level fundamentally and to carry out targeted prevention and treatment.

The tumor microenvironment (TME) in the malignant transformation of gastric cells still needs to be further explored. Among them, tumor-associated macrophages (TAMs) are considered to be key coordinators of tumorigenesis; play an essential role in tumor development [4, 5]; represent the new identity of macrophages after tissue carcinogenesis; and are differentiated into classical activation type (M1) and alternate activation type (M2). The TME is mainly characterized by hypoxia and weak acidity, so TAMs most have the M2 phenotype at tumor sites. M2-like TAMs exhibit several protumor effects: (1) suppression of the tumor immune response, especially T-cell-mediated cytotoxicity, (2) induction of tumor angiogenesis, (3) facilitation of tumor migration, invasion and metastasis, and (4) enhancement of resistance to tumor chemotherapy and radiation therapy [6–8]. Previous studies have emphasized that macrophages that are activated to the M2 type promote proliferation, invasive metastasis, angiogenesis and drug resistance in GC tumour cells [7, 9]. In addition, the degree of M2-like TAM infiltration in tumor tissue was observed to correlate with prognosis, and patients with a high infiltration of highly expressed CD163 + M2-like TAMs had a low survival rate [10]. However, the prognosis of GC patients is poor and heterogeneous, and there is an urgent need for effective therapeutic targets and more accurate prognostic assessment methods. Therefore, exploring specific risk signatures associated with M2-like TAMs that can identify GC cases and generate relevant personalized treatment regimens to improve efficacy is a promising strategy for tumor immunotherapy.

Here, we used the weighted gene co-expression network analysis (WGCNA) of two transcriptomic datasets to screen the central modules most associated with M2-like TAMs. Then, differential analysis, prognostic correlation analysis, and LASSO-Cox regression were performed to obtain M2-like TAM-related genes with prognostic value; four of these genes, SERPINE1, MATN3, CD36 and CNTN1, were screened as M2 macrophage-related prognostic markers. An M2-like TAM-related risk signature was constructed and could be used to guide clinical use of drugs with important implications for prolonging survival in GC patients. Patients were grouped into high- and low-risk groups according to the optimal cut-off value (risk score = 1.4). Our results demonstrate differences in the immune landscape and immune response in high- and low-risk populations and indicate potentially effective anticancer agents for these populations. The flow chart for this study is shown in Fig. 1.

2 Materials and methods

2.1 Data collection and processing

Sequencing profiles of GC tissues and normal tissues were obtained from The Cancer Genome Atlas (TCGA) database and the GEO dataset GSE84437. Next, the TCGA-STAD dataset (containing clinical information and survival data of 443 GC patients) was employed for signature construction. Survival data for TCGA-STAD were extracted from UCSC Xena database. Gene expression data were obtained by converting FPKM to TPM. The clinical information, gene expression data and survival data for 433 GC patients in the GSE84437 dataset (the test set) were obtained and normalized using the “GEOquery” R package [11].

2.2 Identification for M2-like TAM-related genes

The relative content of TAMs was calculated by the CIBERSORT algorithm using gene expression data [12]. The weighted coexpression network was generated using the WGCNA method [13], and the expression data from GSE84437 and TCGA-STAD were assessed to obtain the genes most associated with M2-like TAM content. Then, using the CIBERSORT results

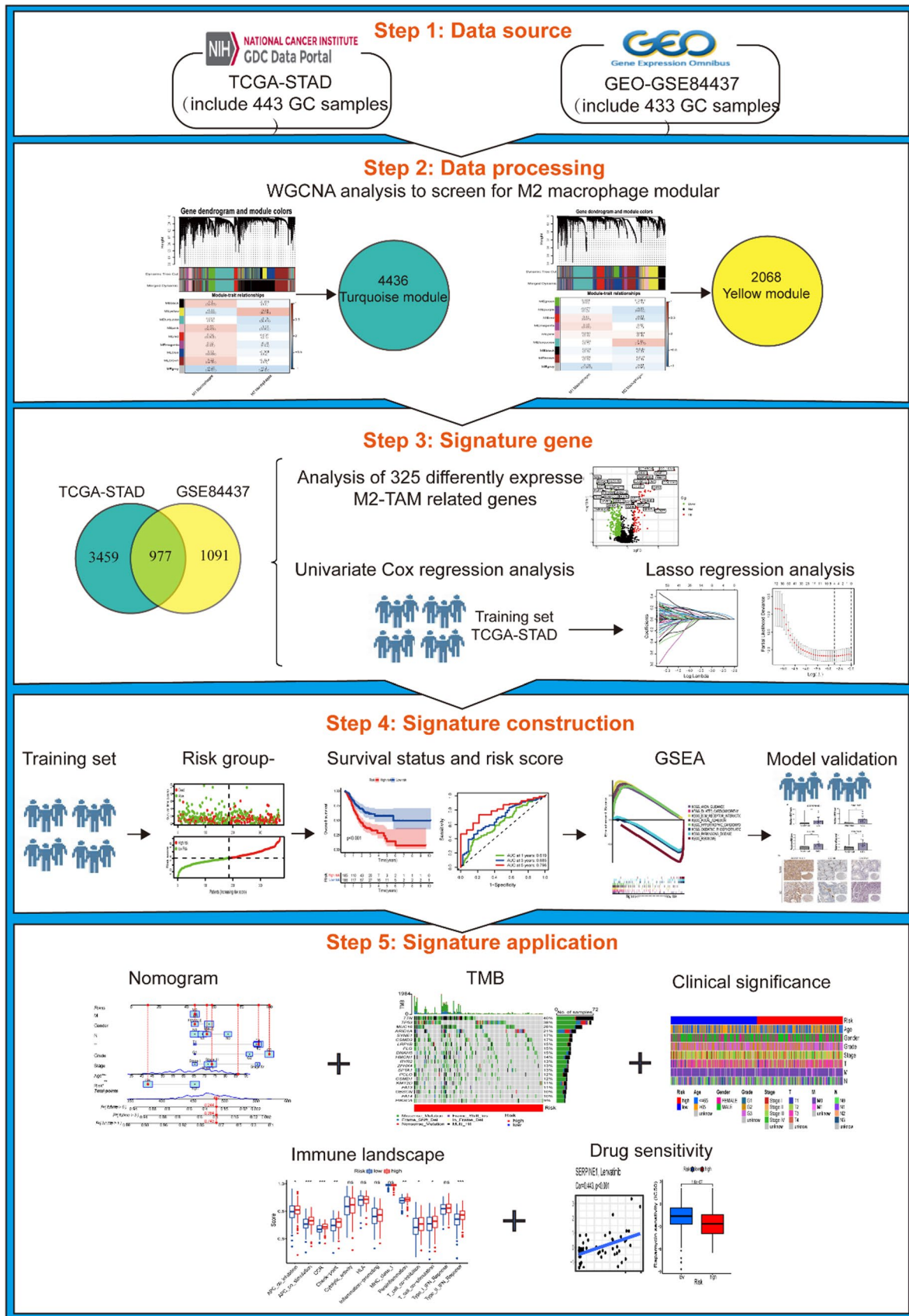


Fig. 1 The flow chart of this study

as the sample phenotype, outliers were excluded, and the network established with setting a suitable soft threshold power (β) reaches the scale-free network standard. All genes were divided into several modules, and the modules with higher similarity were merged using the “dynamic tree cutting” algorithm, and the minimum number of genes/module was set to 50. Next, Pearson correlation analysis was conducted between modules and traits as a way to identify the module most closely related to M2-like TAM content. Finally, module genes obtained from both datasets were extracted and intersected to screen for M2-like TAM-related genes.

2.3 Establishment and validation of prognostic signature

To explore the prognostic role of M2-like TAM genes, a prognostic signature was constructed and validated. First, univariate Cox regression analysis was used to screen prognosis-related candidate signature genes. Next, we further filtered feature genes based on the “survival”, “glmnet” and “timeROC” packages for LASSO regression analysis. The patient risk score was calculated based on the gene expression level and its corresponding coefficient according to the following formula: $Risk\ score = \sum_{i=1}^n [Coefficient(i) * expression(i)]$. Then, the TCGA cohort’s patients were separated into two groups, high- and low-risk groups, according to the optimal cutoff of the risk score. Kaplan-Meier testing was applied using the “survminer” R package for the high- and low-risk groups to assess the difference in survival rates between the two groups. In addition, the “timeROC” R package was applied to plot ROC curves to assess the predictive stability of the signature genes. Univariate and multivariate Cox regression analyses were performed to exclude the effects of multiple covariates and to assess the performance of signature independent prognostic indicators. Pathway analysis was performed using gene set enrichment analysis (GSEA) to identify pathways and biological processes involved in differential gene sets in the high- and low-risk groups of the TCGA cohort [14]. The gene set alignment operation was performed 1,000 times in each analysis, and $FDR < 0.25$ and $p < 0.05$ were used as screening criteria for significantly enriched marker gene sets and KEGG pathways. Subsequently, in the set GSE84437, nomogram, calibration curves, and risk curves were plotted in conjunction with clinical data and risk score to assess the prognostic signature for validation.

2.4 Collection and processing of somatic alteration data

Tumor mutation burden (TMB) was considered to be a marker for predicting response to tumor immunotherapy, and those with high TMB responded better to immunotherapy [15]. Gene mutation data of GC patients were obtained from TCGA database, and the genomic mutations in tumor samples were analyzed by using the R package “maftools” [16], and the samples were grouped into two groups, labeled as low-TMB and high-TMB groups, using the median TMB value as the cut-off point. The difference in survival rates between the two groups was then analyzed using the R package “survival”.

2.5 Risk signature-related immune landscapes

The CIBERSORT algorithm was used to analyze the proportion of 22 tumor-infiltrating immune cells in the high- and low-risk groups as a way to assess and compare the composition of tumor-immune infiltrating cell types and differences between groups [17]. The correlation between risk score of prognostic signature and common immune checkpoints was also analyzed. TME score was performed by applying the ESTIMATE algorithm. Next, the Tumor Immune Dysfunction and Exclusion (TIDE) score was used for analyzing the effectiveness of immunotherapy [18].

2.6 Drug correlation analysis and drug screening

To further explore more effective therapeutic targets and drugs, drug assay data from the CellMiner database were employed to select antitumor agents for which sensitivity was significantly correlated with the expression of the risk signature genes [19]. In addition, based on the GDSC database, the gene expression profile of GC samples, and the information on risk groups, drug half-maximal inhibitory concentration (IC50) values were calculated via the R package “pRRophetic” [20]. A lower IC50 value indicates that the drug has better therapeutic effect and anti-cancer sensitivity.

2.7 Clinical sample collection, mRNA and protein expression analysis of signature genes

GC tissues and normal paracancerous gastric tissues were collected from 13 GC patients in Xijing Hospital (Xi’an, China), and all specimens were clearly diagnosed by pathological examination and the patients signed a written informed

consent form. All methods were carried out in accordance with the institutional guidelines and regulations. The expression of prognostic signature genes in the tissues was verified by qRT-PCR. Total RNA was extracted from fresh tissues using Trizol reagent (Life Technologies), first-strand cDNA was synthesized according to Prime Script RT reagent Kit (Invitrogen), and qRT-PCR was performed using Power SYBR™ Green PCR Master Mix (Invitrogen). The signature gene primer sequences were in Additional file 1: Table S1. The $2^{-\Delta\Delta C_t}$ method was used to calculate the relative expression of target genes. And protein expression of M2-like TAMs signature genes in GC tissues was analyzed in the Human Protein Atlas database (<http://www.proteinatlas.org>), which provides immunohistochemical micrographs of GC and paired paracancerous tissues.

2.8 Statistical analysis

The R software version 4.0.3 and GraphPad Prism 8.3.0 were used for statistical analysis. Survival curves were compared using the Kaplan-Meier method and Log rank test. $p < 0.05$ was considered a statistically significant difference.

3 Results

3.1 Construction of WGCNA and identification of hub modules

To further illuminate the relationship between TAMs and prognostic survival in GC, WGCNA was performed for the GSE84437 and TCGA-STAD cohorts. A scale-free network was constructed, and set the soft threshold power (β) to 9 for GSE84437 (Fig. 2a), and the soft threshold power (β) for TCGA analysis was set to 8 (Fig. 2c). Genes with similar expression patterns were introduced into the same module by dynamic tree-cutting algorithm, making a hierarchical clustering tree with different modules. Hierarchical clustering analysis was performed according to weighted correlation, and the clustering results were segmented based on the set criteria to obtain 9 gene modules, respectively (Fig. 2b and d). Each column of Fig. 2e and f presented the 2 tumor-infiltrating immune cells types, and each row presented the candidate module with traits vector genes. For TCGA-STAD, it was worth mentioned that the turquoise module was highly correlated with M2 Macrophages ($Cor = 0.25$, $p = 4e-05$, Fig. 2f) among 9 candidate modules. For GSE84437, the yellow module had the strongest positive correlation with M2 Macrophages ($Cor = 0.28$, $p = 4e-09$, Fig. 2e) among 9 candidate modules. Our primary concern was the M2 Macrophages, and so we fetched the genes in the turquoise and yellow modules for further research.

3.2 Screening of prognostic signature genes

A total of 4436 and 2068 genes were integrated into the yellow and turquoise modules, respectively. The intersection of the two modules was determined, and 977 candidate M2-like TAM-related genes were screened and visualized by a Venn diagram (Fig. 3a). Among these M2-like TAM-associated candidate genes, there were 325 differentially expressed genes (Fig. 3b, Table S2), of which 86 were downregulated and 239 were upregulated ($FDR < 0.05$, $|\log_2FC| > 1$). We then further analyzed the prognostic valence of the candidate genes by mining the expression data in the TCGA-STAD dataset. Initially, the results showed that 119 genes were associated with GC prognosis by univariate Cox regression analysis (Figure S1). Finally, further screening variables were analyzed by LASSO regression, and 4 signature genes were obtained (Fig. 3c and d): SERPINE1 (serpin family E member 1), MATN3 (matrilin 3), CD36 (CD36 molecule), and CNTN1 (contactin 1). Differences in clinicopathological features and gene expression profiles between two clustered subgroups visualized by heatmap (Fig. 3e).

3.3 Construction of a signature based on M2-like TAM-related genes

The risk score for all samples were calculated by the expression levels of signature genes and correlation coefficients in the TCGA-STAD dataset. Construction of a risk score signature: $Risk\ score = (0.10748076 * SERPINE1) + (0.08583133 * MATN3) + (0.02872120 * CD36) + (0.03888511 * CNTN1)$. GC patients were grouped into high- and low-risk groups according to the optimal cut-off value (risk score = 1.4) (Fig. 4a). The results showed higher overall survival (OS) in the low-risk group than in the high-risk group (Fig. 4b), and similarly, DFS, PFS and DSS analyses showed a poorer overall prognosis in the high-risk group (Figure S2a–c). The ROC curve used to evaluate

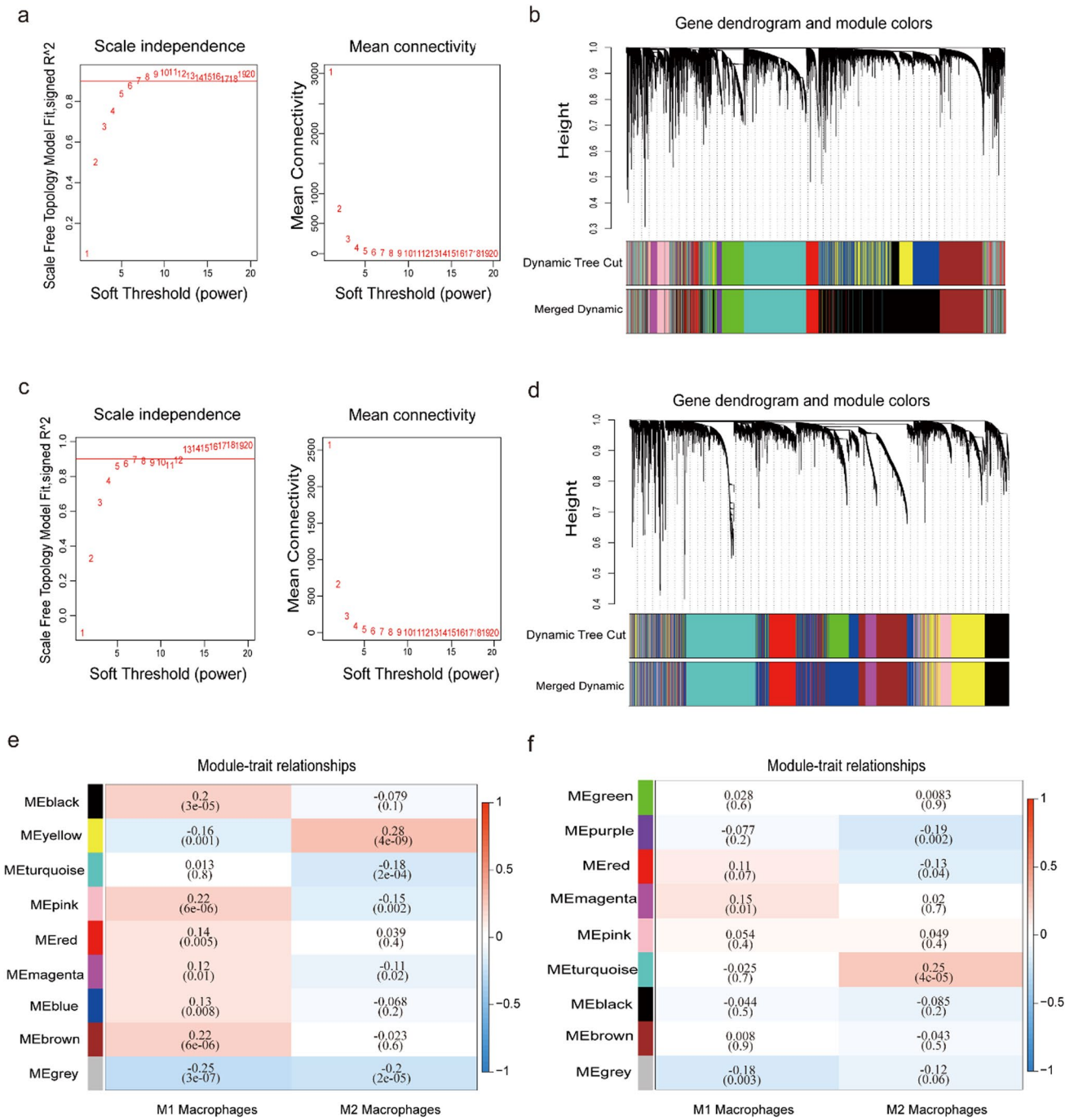


Fig. 2 Establishment of the networks via WGCNA. **a, c** The optimal soft threshold power (β) of GSE84437 was set to 9, and the soft threshold power (β) of TCGA was set to 8. **b, d** A clustering dendrogram displayed similar expression patterns of genes clustered into coexpression modules in TCGA-STAD and GSE84437. **e, f** The heatmap demonstrated the correlation between modules and traits (immune infiltrating cells), with the yellow and turquoise modules identified as the highest correlated modules for M2-like TAMs.

the sensitivity and specificity of the prognostic signature also demonstrated the good predictive ability of the signature, with AUC of 0.796 for 5-year OS (Fig. 4c). Then, the univariate Cox regression results showed the risk ratio (HR) of 7.495 (95% CI 3.424–16.409; Fig. 4d) for the risk score was associated with prognosis; multifactorial Cox regression results showed that risk score was a significant predictor at an HR of 7.033 (95% CI 3.138–15.763; Fig. 4e), and the C-index results also showed a better performance in prediction accuracy of prognostic signature (Fig. 4f). Moreover, GSEA showed that the KEGG signaling pathway in the high-risk group was mainly enriched in “Axon guidance”, “Dilated cardiomyopathy”,

"Hypertrophic cardiomyopathy hcm", "Ecm receptor interaction" and "Focal adhesion", whereas the low-risk group was mainly involved in metabolic-related pathways such as "Oxidative phosphorylation" (Fig. 4g).

3.4 Validation of prognostic signature

Next, we performed further validation in the test set GSE84437 to verify the validity and improve the generality of the prognostic signature. The test set was divided into high-risk and low-risk groups by setting the thresholds in the same way (Fig. 5a), and the survival curves of the two groups were plotted and the difference in survival was tested by Log-rank, which showed that patients with high-risk score had a poor prognosis, and the difference in prognosis between high- and low-risk score was significant (Fig. 5b). The ROC curve showed AUC values of 0.600, 0.622 and 0.607 for OS at 1, 3 and 5 years, respectively, which also demonstrated the good prognostic ability of this signature (Fig. 5c). Furthermore, the results of calibration curve and ROC curve of the nomogram indicate that the signature was reliable and accurate in predicting the prognosis of GC patients (Fig. 5d, f).

3.5 The prognostic value of TMB in GC

Recently, an increasing number of studies have shown that TMB is a novel biomarker for immune checkpoint inhibitors (ICIs), which can predict the efficacy of immunotherapy [15]. Our results showed that TMB levels were higher in the low-risk group than in the high-risk group ($p = 2.3e-06$, Fig. 6a), and that patients with high TMB had a better prognosis than those with low TMB ($p < 0.001$, Fig. 6b). A further correlation analysis showed that the risk score was negatively correlated with TMB level ($R = -0.26$, $p = 3.8e-07$, Fig. 6c). Recent studies have highlighted that among cancer patients receiving immunotherapy, those with high TMB have better immunotherapy efficacy and that high TMB is associated with better survival [21–23]. To further explore the validity of the prognostic significance of the risk score and TMB, we validated the effect of both indicators in the prognostic prediction of GC. Stratified survival curves showed that risk score subgroups exhibited significant prognostic differences between low and high TMB status, and that those in the high-risk group with low TMB levels had a worse prognosis (Fig. 6d), suggesting that in addition to TMB, risk score is an independent prognostic factor for patients with GC. Additionally, the distribution of mutations in the high-risk group (total mutation rate of 83.98%) and low-risk group (total mutation rate of 92.27%) was visualized using waterfall plots (Fig. 6e and f). The mutation rates of TTN (40%) and TP53 (38%) were greater than 30% in the high-risk group, and the mutation rates of TTN (54%), TP53 (45%), MUC16 (33%), and LRP18 (33%) were higher than 30% in the low-risk group. These results revealed the correlation between M2 tumor-associated macrophage infiltration and the efficacy of GC immunotherapy from the perspective of somatic cell variation level, which could be suggestive for the prognosis of patients and the prediction of the efficacy of immunotherapy.

3.6 Correlation of prognostic risk signature with clinical parameters

Next, clinicopathological analysis was performed to explore the relationship between clinical parameters and risk score (Fig. 7a). Based on clinicopathological indicators, GC patients were divided into different subgroups for survival analysis, and the results showed that the risk score still predicted the prognosis of patients by age, and the higher the risk score the worse the prognosis (Fig. 7b and c). Consistently, the risk score showed strong prognostic predictive power for male or female patients (Fig. 7d and e), patients with G1-2 or G3 grade tumors (Fig. 7f and g), patients with T1-2 or T3-4 stage (Fig. 7h and i), and patients with N0 or N1-3 status (Fig. 7j and k). These results suggest that the M2-like TAM risk score correlates with the clinicopathological characteristics of GC patients.

3.7 Risk signature-related immune landscape analysis

Based on the CIBERSORT algorithm, the proportion of 22 immune cell types in GC patients was calculated and compared between the high-risk and low-risk groups (Fig. 8a), and statistically significant differences were found between 4 immune cell types ($P < 0.05$), resting NK cells, M2 macrophages, plasma cells, and activated dendritic cells. The results of immune function analysis by the ssGSEA algorithm in the high- and low-risk groups showed significant differences in the APC co-inhibition, APC co-stimulation, CCR, checkpoint, parainflammation, T-cell co-inhibition, T-cell co-stimulation, and type-II IFN response scores (Fig. 8b). Correlation analysis of 4 signature genes (CD36, CNTN1, MATN3, SERPINE1) with 22 immune cells revealed that each signature gene was positively correlated with M2 macrophages (Fig. 8c). Moreover, the

Fig. 3 Identification of M2-like TAM-associated prognostic genes. **a** Venn diagram showing the shared genes of TCGA-STAD (turquoise module) and GSE84437 (yellow module). **b** Volcano plot demonstrating the distribution of differentially expressed genes shared in the yellow and turquoise modules. **c, d** LASSO regression analysis to screen signature genes. **e** The heatmap displays the distribution of the two clustered subgroups in terms of gene expression and clinicopathological characteristics

TME score results showed that stromal components and immune cells were higher in the high-risk group of GC patients (Fig. 8d), suggesting that patients had lower tumor purity. For immunotherapy, the higher TIDE value in the high-risk group indicated that patients in the high-risk group had a poorer response to immunotherapy and were more likely to evade the immune system (Fig. 8e).

3.8 Drug sensitivity analysis

The expression of signature genes was correlated with drug sensitivity based on cellminer analysis. The results revealed a positive correlation between MATN3 expression and dacomitinib sensitivity (Fig. 9a), and the results demonstrated that SERPINE1 expression was positively correlated with simvastatin sensitivity (Fig. 9b). Additionally, the lower IC50 values for 10 chemotherapeutic agents, including rapamycin, thapsigargin, A-770,041, bexarotene, bryostatin 1, cyclophosphamide, imatinib, lapatinib, midostaurin and sunitinib in the high-risk group, suggesting that these 10 chemotherapeutic drugs would be more effective and require lower concentrations in the high-risk group (Fig. 9c-l). Moreover, thapsigargin had the lowest IC50.

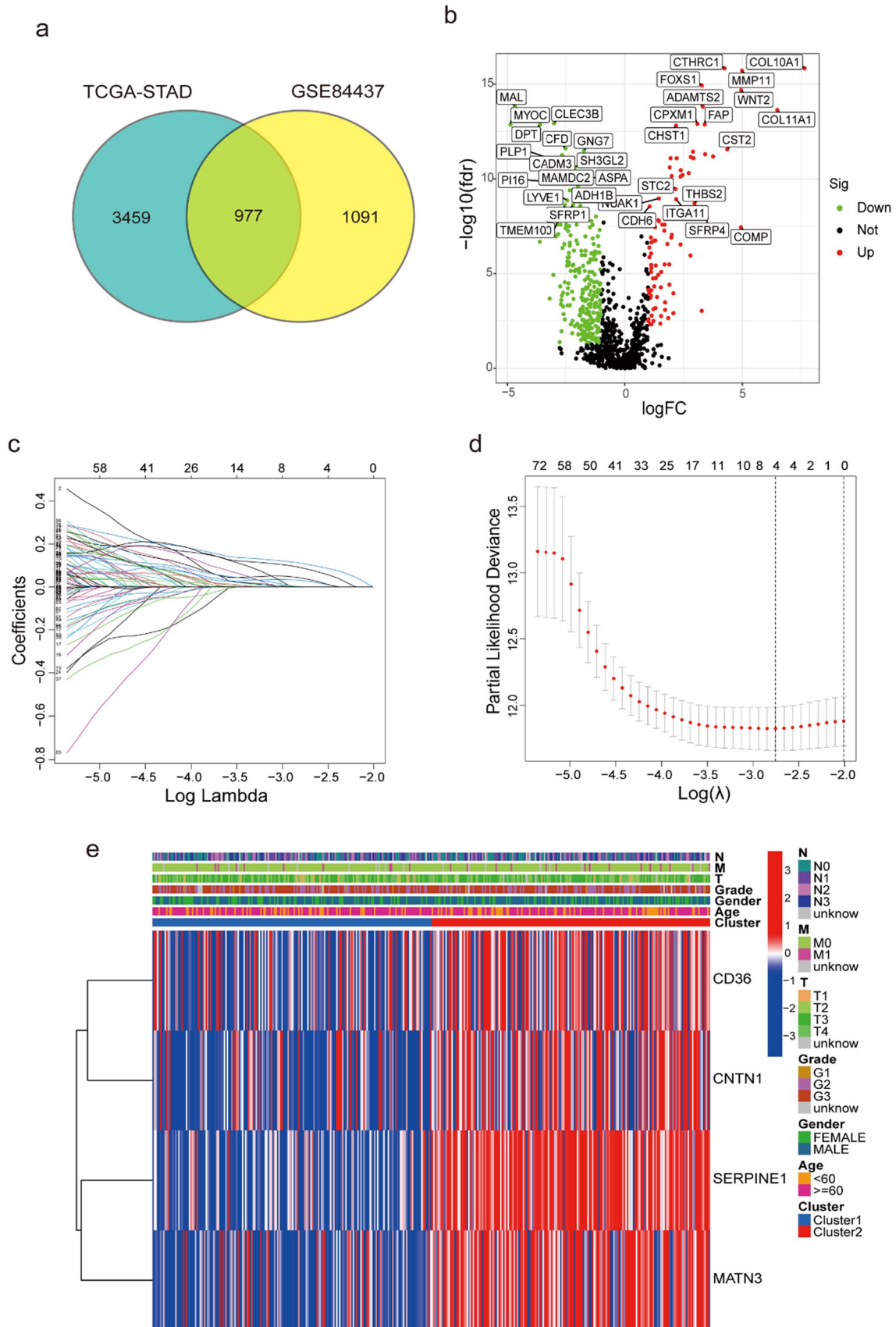
3.9 Expression of signature genes in tissues by qRT-PCR and IHC

We analyzed 13 pairs of GC tissues and paracancer controls and verified the mRNA levels of four genes. The results showed high expression of SERPINE1, MATN3, CD36 and CNTN1 in GC tissues (Fig. 10a). Except for MATN3, which is not available in the HPA database, we explored the protein expression of other M2-like TAMs-associated signature genes in GC tissues (Fig. 10b). The trend of our experimental results is generally consistent with the data analysis.

4 Discussion

Accurately predicting the prognosis and risk classification of cancer patients is related to the choice of treatment plan and has a direct impact on the outcome of treatment [4]. Jae-Ho et al. constructed a 32-gene signature from gene expression data of 567 GC patients [24], and Jae Yong Cho et al. developed a gene expression scoring system based on six recurrence-related gene expression scores by analyzing gene expression profile data of 65 GC patients [25]. Another study constructed a multiple pathologic signature based on hemoglobin and eosin-stained slides from a pathologic perspective and may be a potential predictor for adjuvant chemotherapy decisions [26]. Although researchers have been trying to construct models that can predict the prognosis of GC patients, the results are often unsatisfactory due to the high heterogeneity of malignant tumors. Currently, M2-like TAMs have become a new target for individualized treatment of malignant tumors, and to the best of our knowledge there is a lack of studies to construct GC-related prognostic signatures from the perspective of TAMs to reveal the immune profiles.

Tumor-associated macrophages (TAMs), the most abundant immune cells in the tumor microenvironment (TME), can be differentiated into M1 and M2 types, which have become new therapeutic targets and prognostic indicators in the individualized treatment of malignant tumors [7, 27, 28]. TAMs isolated from tumor-bearing mice and human tumors usually have the M2 phenotype; previous studies have reported that the level of M2-like TAMs correlates with peritoneal metastasis of GC, and the results of detecting ascites or peritoneal lavage showed that the level of M2-like TAMs was significantly higher in patients with peritoneal metastasis of GC than in patients without metastasis [9, 29, 30]. A high density of M2 macrophages was found to be associated with poorer overall survival in a variety of malignancies, including GC [31, 32]. Zheng, P. et al. showed that M2 macrophage-derived exosome-mediated ApoE promotes GC cell invasion and metastasis in vivo and in vitro [33]. The above results emphasize that a large number of TAMs polarized to M2-type macrophages in tumor tissues protects tumors from immune surveillance, which in turn promotes tumorigenesis, invasion and metastasis. Although current GC treatments are becoming more diverse, with many breakthroughs in combining targeted therapies with immune checkpoint inhibitors, this diversity underscores the importance of personalized assessment methods. However, the mining of reliable markers for screening for precision targeted therapy to prolong



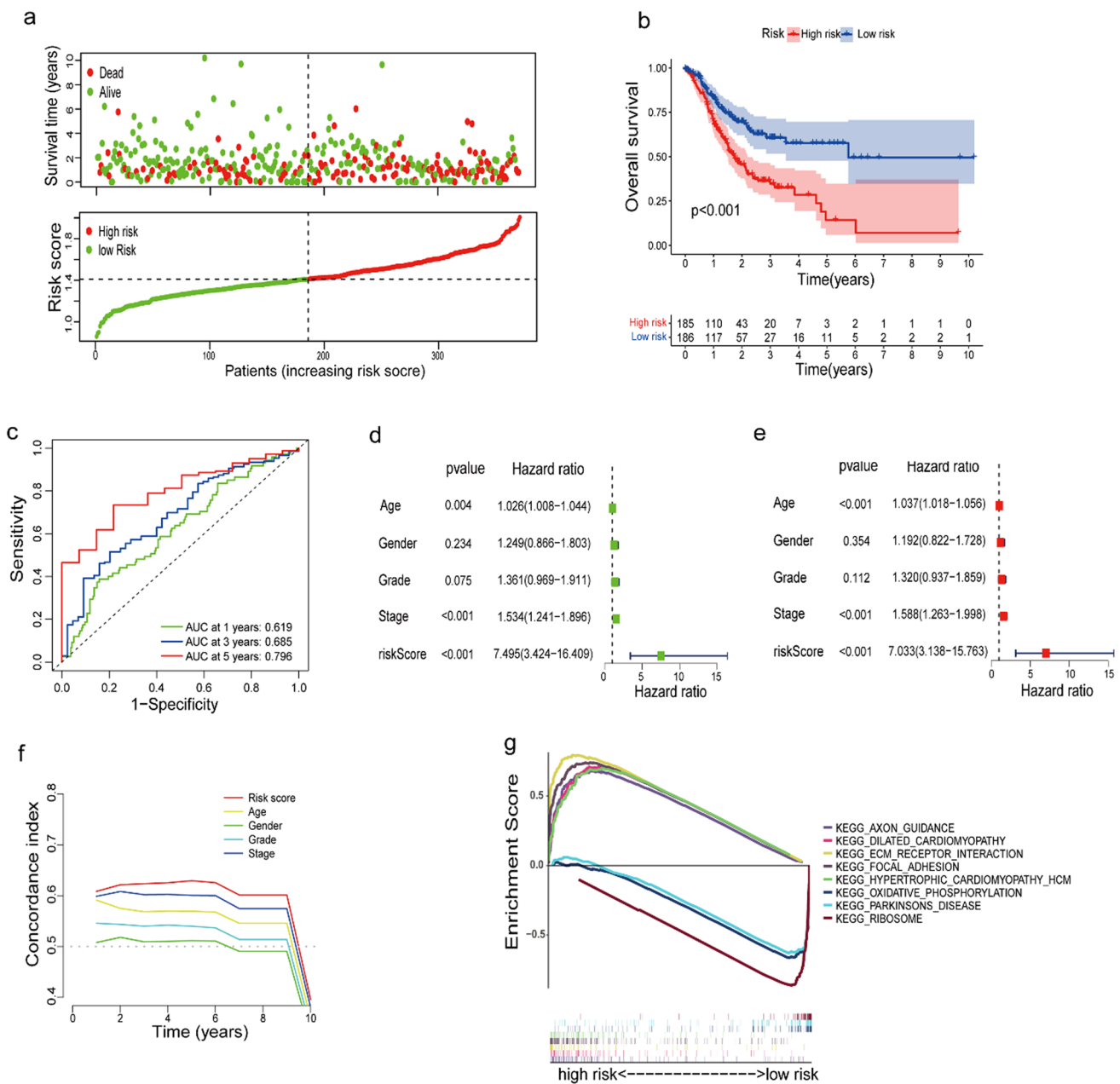


Fig. 4 Establishment of the prognostic risk signature. **a** Survival status and risk score for GC patients in the low- and high-risk groups. The black dashed line is the optimal cutoff value for classifying patients into low- and high-risk groups. **b** Kaplan–Meier curve analysis showed the difference in overall survival between the low- and high-risk groups. **c** ROC curve and AUCs of the risk score model at 1, 3, and 5 years. **d–f** Univariate Cox regression, multivariate Cox regression and C-index analyses showed that the risk score was an independent risk factor in terms of survival and was superior to other indicators. **g** GSEA results demonstrated significant enrichment of 8 KEGG pathways in the low- and high-risk groups

the survival of patients with various types of GC still needs to be further explored. Therefore, the exploration of molecular targets with promising predictive effects on prognosis in GC is essential for targeting therapy using M2-like TAMs.

Currently, prognostic signatures for molecular characterization have been widely applied to various diseases, and these signatures can be used to understand the distribution and function of disease-related genes through high-throughput technology, and to analyze the underlying mechanisms of diseases more comprehensively. In this study, multiple computational algorithms based on WGCNA and differential expression analysis were used to mine the M2-type tumor macrophage coexpression network in two GC cohorts: TCGA-STAD and GSE84437. Univariate Cox and LASSO regression analyses were then used to identify M2-like TAM-related genes (SERPINE1, MATN3, CD36 and CNTN1) that

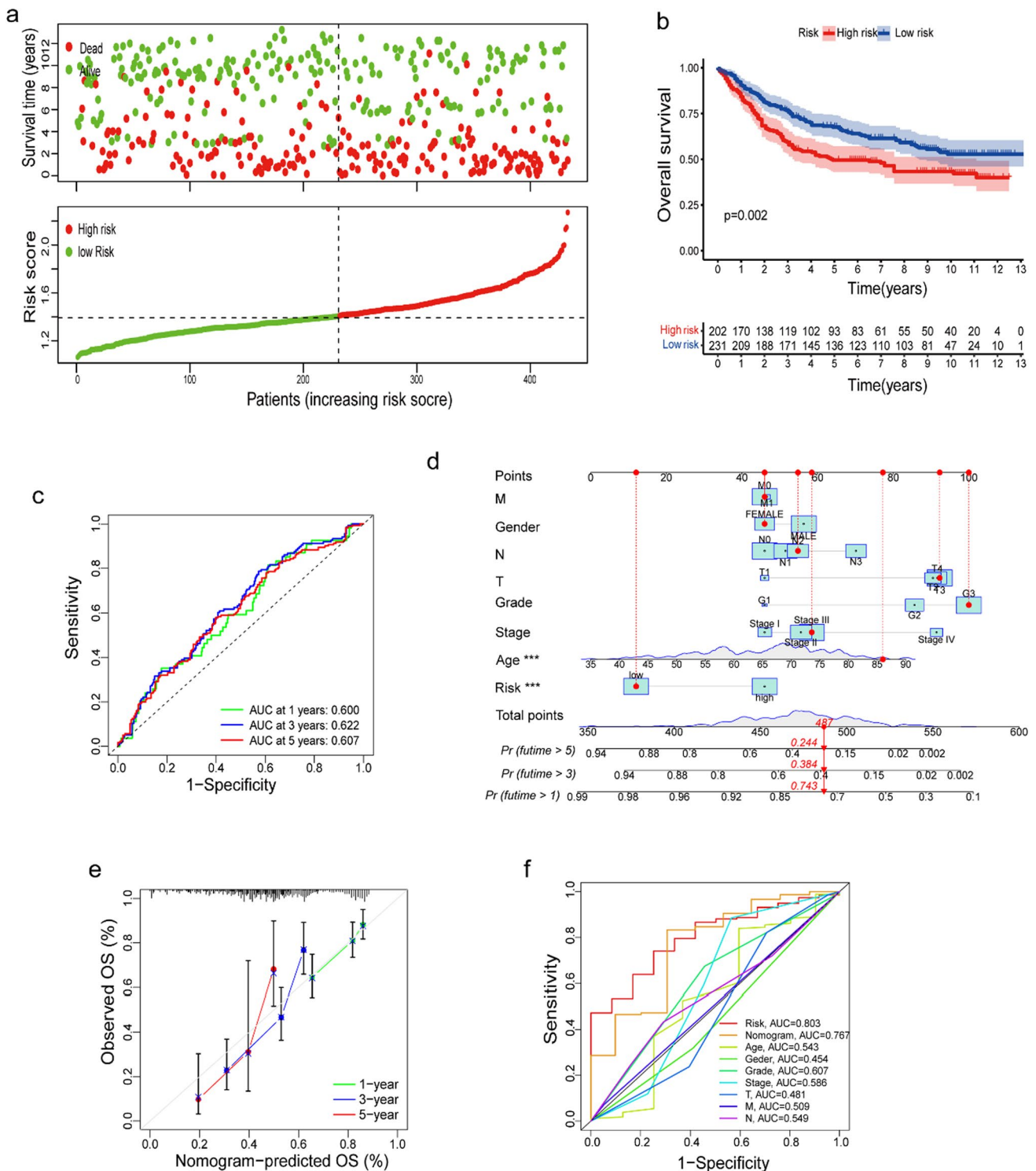


Fig. 5 Validation of the prognostic M2-like TAM-related signature. **a** Survival status and risk score for GC patients in the low- and high-risk groups. The black dashed line is the optimal cutoff value for classifying patients into low- and high-risk groups. **b** Kaplan–Meier curve analysis showed the difference in overall survival between the low- and high-risk groups. **c** ROC curve and AUCs values of the risk score model at 1, 3, and 5 years. **d** A nomogram was constructed to predict the survival of GC patients at 1, 3 and 5 years. **e** 1-, 3-, and 5-year calibration curves of the nomogram. **f** ROC curve analysis of the nomogram

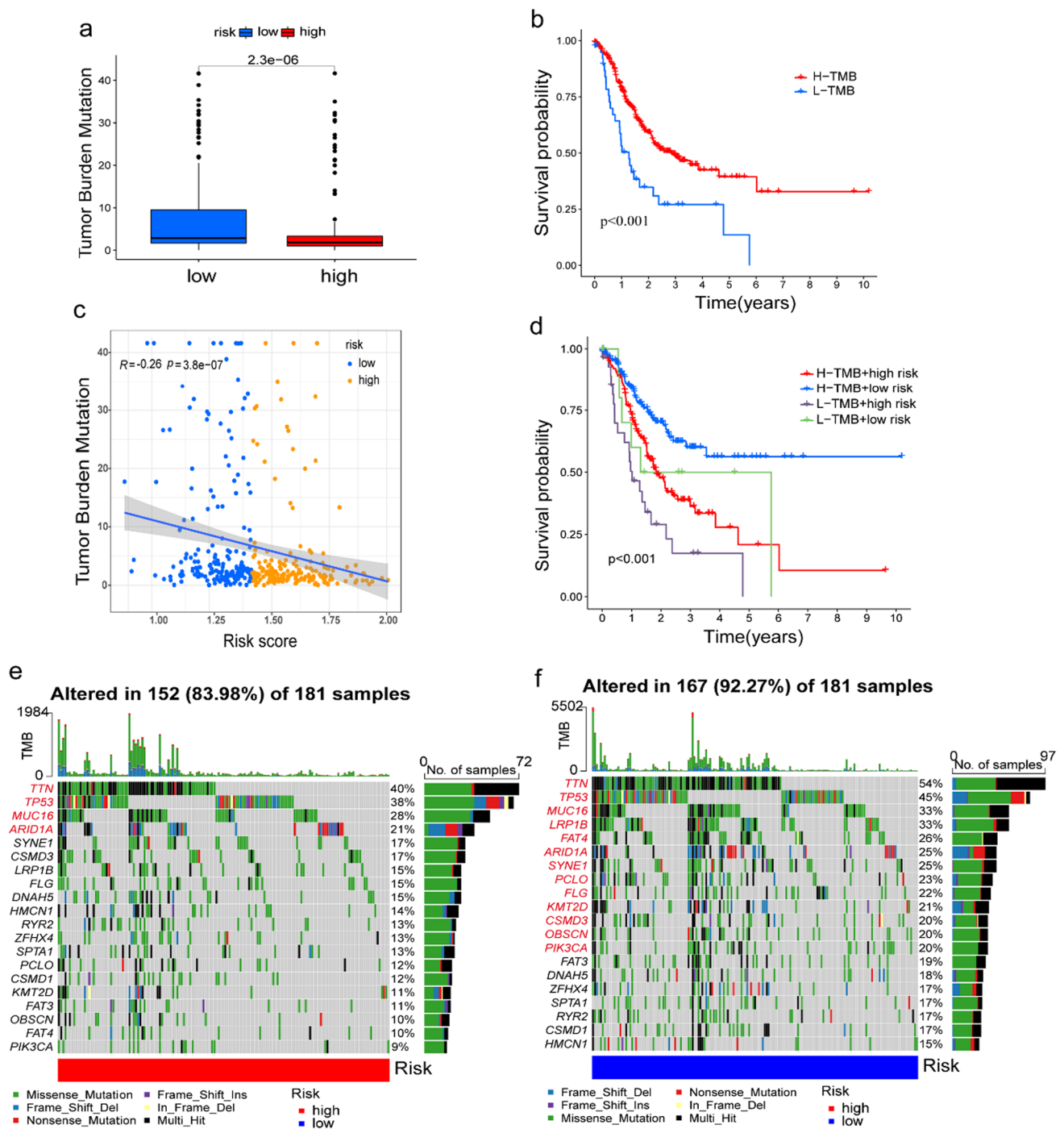


Fig. 6 Correlation of the risk signature with TMB. **a** The difference in TMB between the low- and high-risk groups. **b** K-M curve for the low- and high-TMB groups. **c** Spearman correlation analysis demonstrated a negative correlation between the risk score and TMB. **d** A K-M curve was constructed for patients stratified by TMB and risk score. **e, f** The waterfall plot shows the distribution of the top 20 genes with the highest mutation frequencies in the high- and low-risk score groups

affect the survival of GC patients, and prognostic risk signature was constructed and validated. The four signature genes finally screened in this study have been studied in GC. Chen et al. found that overexpression of SERPINE1 resulted in the development of malignant progression of GC and a poorer prognosis [34]. MATN3, a protein commonly found in the extracellular matrix, was found to predict the prognosis of GC, and the higher its expression in GC tissues, the worse the prognosis of patients [35]. Pan et al. found that CD36 regulates the uptake of exogenous fatty acids by GC cells through activation of AKT/GSK-3β/β-catenin signaling pathway, which induces metastasis and invasion of GC, and also CD36

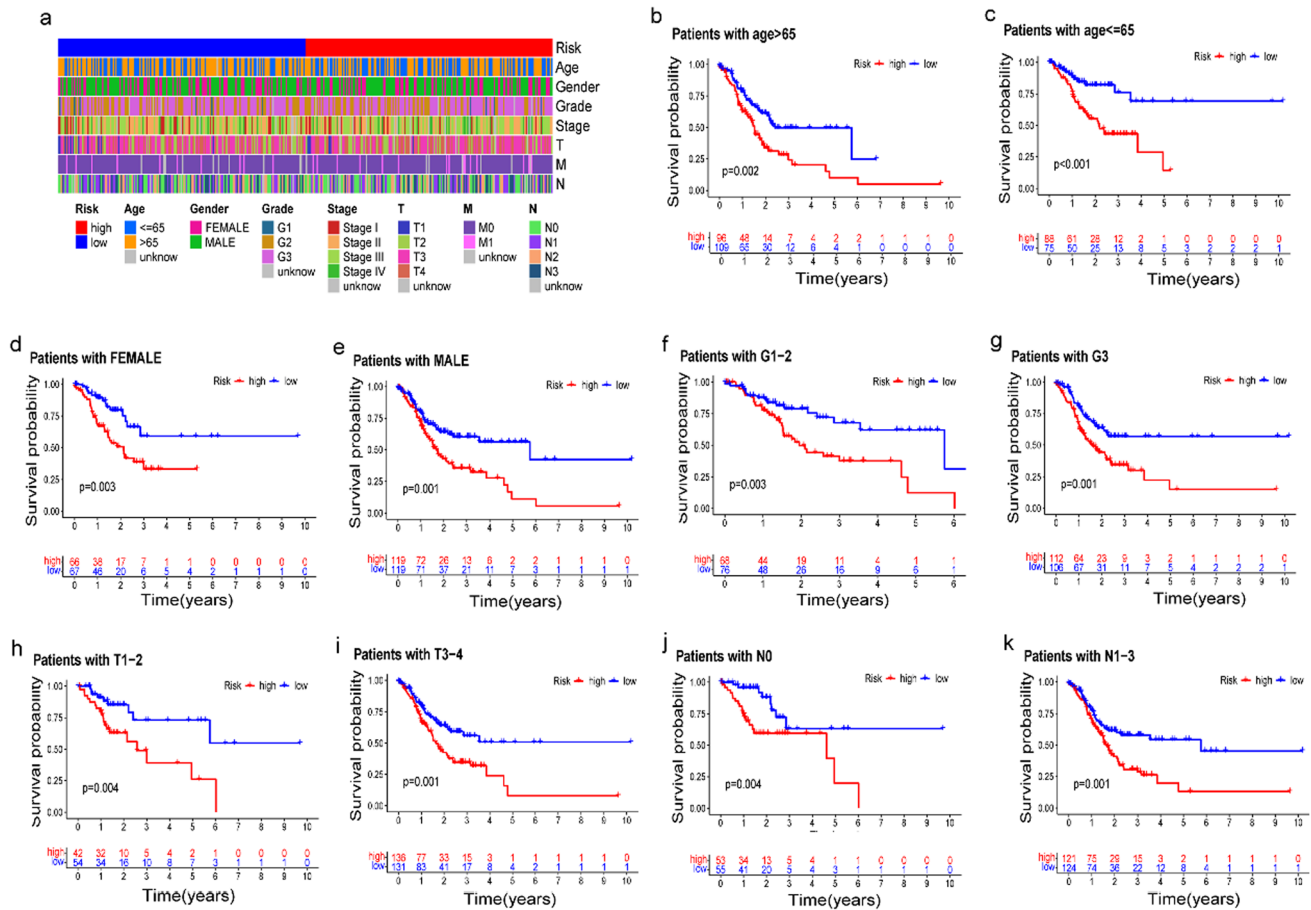


Fig. 7 Prognostic value of clinical characteristics and the risk score. **a** The heatmap displays the distribution of differences in clinical characteristics and corresponding risk scores in the GC patient sample. Kaplan–Meier curves show the results of survival analyses stratified by age (**b, c**), sex (**d, e**), grade (**f, g**), T stage (**h, i**), and N status (**j, k**)

was significantly negatively correlated with the prognosis of GC patients, suggesting that CD36 may become a novel therapeutic target for GC [36]. The expression of CNTN1 protein in primary foci of GC correlated with TNM stage, lymph node metastasis and prognosis of GC patients [37, 38]. Although some studies related to these prognostic genes have been reported, studies on the role of these genes in tumors are still relatively limited, and the related mechanisms and biological significance need to be further investigated. Here we used these genes jointly for the construction of GC prognostic signature, and better typing of GC patients based on the expression of these genes would be beneficial to the clinical decision-making of patients.

Next, ROC curve, C-index, univariate and multifactor analyses showed that our signature could be used as an independent indicator for prognostic determination of survival in GC patients. The risk score was calculated based on the prognostic signature formula, and patients were divided into high- and low-risk groups for survival difference analysis. Moreover, further validation was performed in the GSE84437 dataset. The results suggest that our four-gene prognostic risk signature has high predictive power for survival of GC patients, providing a new idea for precision treatment of GC. Additionally, a nomogram was created and validated based on the risk score and the patient’s clinicopathological indicators to increase the clinical applicability of the signature.

In recent studies, TMB is considered a promising novel biomarker that has attracted increasing attention in improving the efficacy of clinical immunotherapy [15, 39]. TMB level varies among patients with GC and is considered a key determinant of molecular subtyping of GC [40]. High levels of TMB indicate that tumor tissue contains more mutations, which may result in more neoantigens being recognized by the autoimmune system, resulting in stronger autoimmune effects and greater susceptibility to benefit from immunosuppressive therapy. Previous studies showed that higher TMB was associated with better prognosis in GC patients, and high TMB was associated with the effectiveness of immunecheckpoint inhibitors (ICI) therapy and chemotherapy [41]. In the present study, the results showed a negative

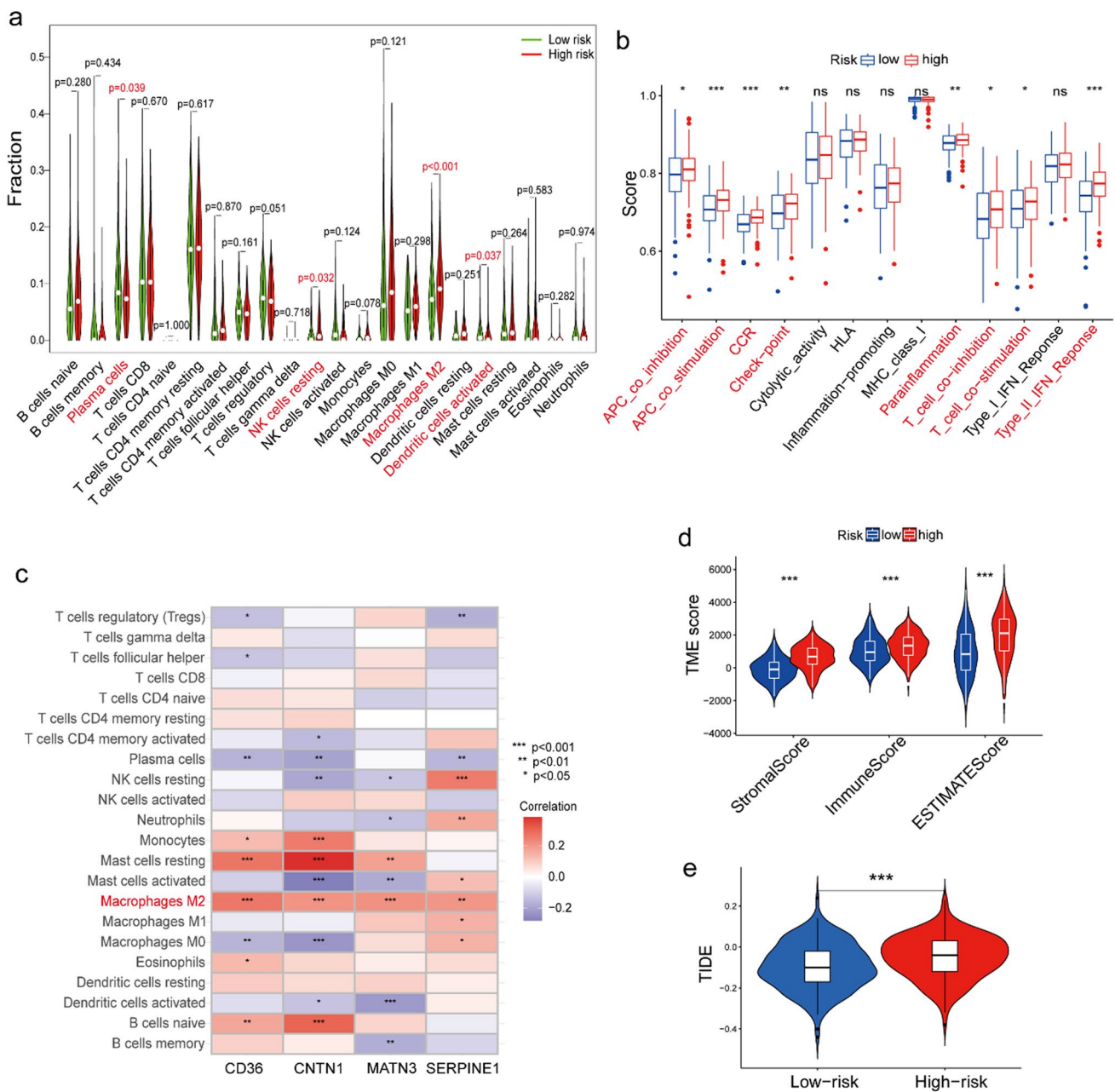


Fig. 8 The prognostic risk signature is associated with the immune landscape. **a** Violin plot demonstrating the difference in immune cell abundance in the low- and high-risk groups. **b** ssGSEA demonstrated differences in immune function in the two risk groups. **c** Correlation of signature genes with immune cells. **d** TME scores of the low- and high-risk groups. **e** The difference in TIDE scores in the two risk groups

correlation between risk score and TMB, with patients in the low-risk group having higher levels of TMB, suggesting that patients in the low-risk group are better able to benefit from ICI treatment.

The prognostic signature constructed in this study also demonstrated the association of high- and low-risk groups with tumor immune infiltration and immunotherapy response. Among the 22 immune cells analyzed, four immune cell types, M2 macrophages, resting NK cells, plasma cells, and activated dendritic cells were significantly different in the high- and low-risk groups. In GC patients, the phenotype of NK cells is suppressed, with reduced numbers, subpopulations, cytokines and cytotoxic effects, while activated NK cells promote antitumor effects [42]. Mimura et al. indicated that in vitro-expanded NK cells have a potent killing effect on GC [43]. The infiltration levels of macrophages differ between normal tissue and tumor tissue, M2-like TAMs have enhanced oxidative phosphorylation and reduced glycolytic pathway metabolism, and patients with higher levels of M2 type in GC tissues have poor prognosis. In patients with resected GC

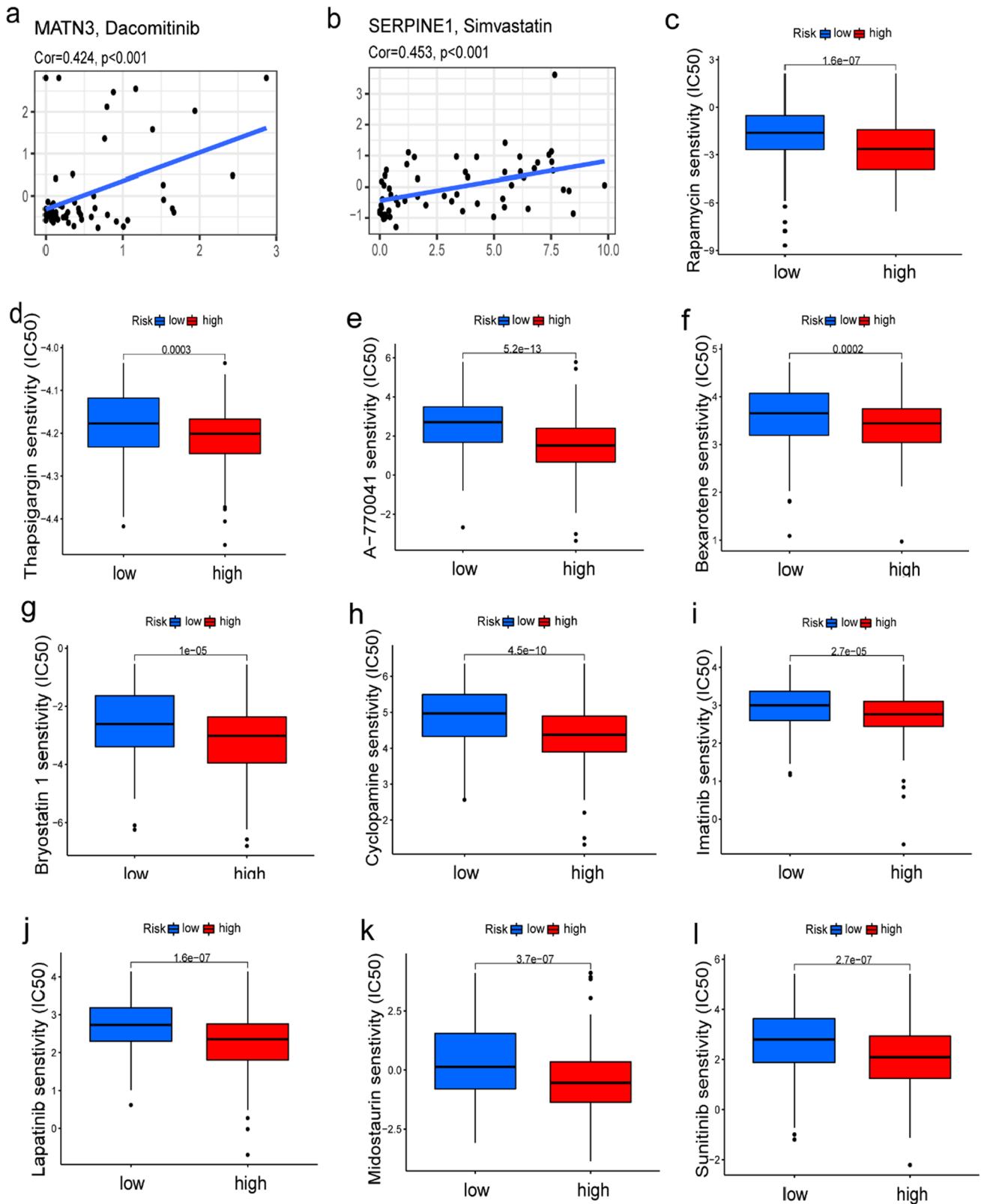
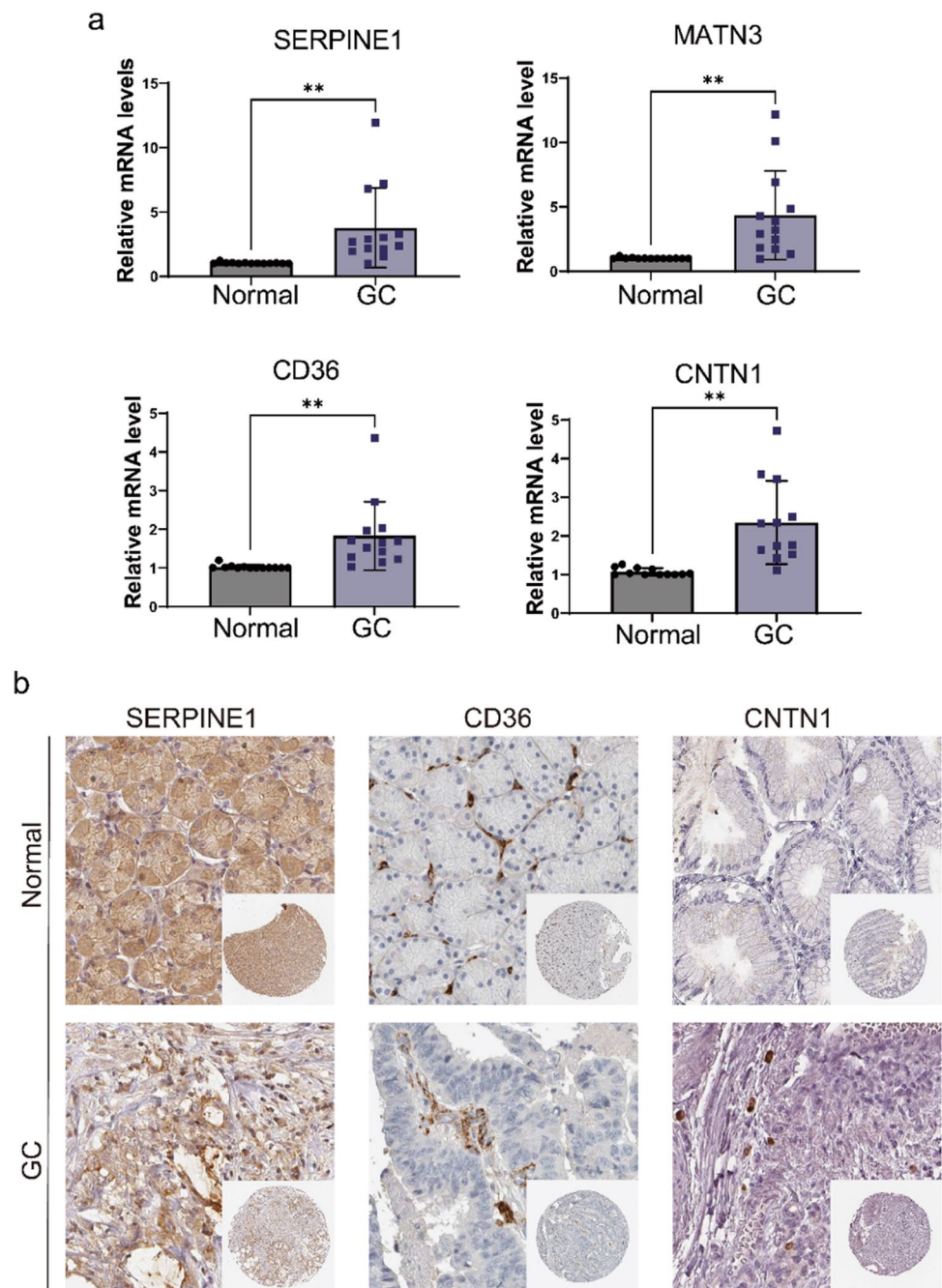


Fig. 9 Drug sensitivity analysis and prediction of potentially effective anticancer drugs. **a** Correlation analysis of MATN3 expression with dacomitinib drug sensitivity. **b** Correlation analysis of SERPINE1 expression with simvastatin drug sensitivity. **c-l** Ten drugs with higher sensitivity in the high-risk group

Fig. 10 Signature genes were analyzed for mRNA expression levels and protein expression distribution. **a** The mRNA expression levels of SERPINE1, MATN3, CNTN1, and CD36 in normal and GC tissues ($n = 13$). **b** Immunohistochemistry showed protein expression of SERPINE1, CD36 and CNTN1 based on the Human protein Atlas (HPA) database



with lymph node metastases, M2 macrophages are also correlated with worse overall survival [44]. In regard to immune function, analysis of ssGSEA-based immune function scores showed significant differences between the two risk groups in response scores such as APC co-stimulation, T-cell co-stimulation and CCR. Moreover, TME scores showed that stromal components and immune cells were higher in the high-risk group of patients, indicating that GC patients had less tumor purity. And the higher TIDE value in the high-risk group indicated that the GC patients in this group had a worse response to immunotherapy. These results revealed a correlation between M2-like TAM-based signature and the immune status of GC and correlated with a distinct immune cell ratio. Crosstalk between M2-like TAMs and neighboring cells is strongly associated with GC progression and treatment resistance [45–47].

In identifying signature genes and performing risk grouping, we predict the therapeutic response of patients in high- and low-risk groups to common anticancer drugs, providing a new idea for a clinical antitumor drug combination approach. We found that the sensitivity to dacomitinib and simvastatin was positively correlated with MATN3 and

SERPINE1 expression, respectively. Dacomitinib has significant antitumor effects, and a phase II clinical study found that dacomitinib was used as a single agent with a tolerable safety profile in patients with HER2-positive GC [48, 49]. Previous studies have found that simvastatin inhibits tumor cell growth by inhibiting the mevalonate pathway, exerting antiangiogenic effects, inducing apoptosis, and repressing tumor metastases [50, 51]. Huang et al. reported that simvastatin combined with DNA methyltransferase inhibitors enhanced simvastatin-induced proliferation inhibition and heat apoptosis in GC cells by modulating the caspase-3/GSDME pathway [52]. Thus, our drug sensitivity data further support that the use of dacomitinib and simvastatin for clinical intervention of GC has good prospects in the future. In addition, the interactions and mechanisms of action between these two drugs and the signature genes deserve further in-depth exploration. The anti-GC drugs were analyzed to predict the most effective drugs in patients, among which rapamycin, thapsigargin, A-770,041, bexarotene, bryostatin 1, cyclopamine, imatinib, lapatinib, midostaurin, and sunitinib had lower IC50 values in the high-risk group, suggesting that these 10 chemotherapeutic drugs were more effective in the high-risk group and exhibited potentially superior anticancer properties. Among them, thapsigargin had the lowest IC50 value. Finally, we verified the expression of four signature genes at the mRNA and protein levels, and the results were generally consistent with our analyzed data.

5 Conclusions

We screened and constructed a signature containing four M2-like TAMs genes, which has a good predictive value for GC prognosis and a novel role in revealing TME features. To our knowledge, this is the first report to construct an M2-like TAM-related signature for GC. The study provides a theoretical basis for the development of personalized treatment plans for GC patients, which is expected to further improve patient survival.

Author contributions XZL and XDQ designed the research. NW and SBL interpreted the data and performed the experiments. XYZ and KXL helped with experiments. XZL wrote the manuscript. SYQ revised the manuscript. All authors reviewed and approved the submission of the manuscript.

Funding This research was supported by National Natural Science Foundation of China (No. 82170560 to YQS), Shaanxi Health Scientific Research Innovation Team Project (No. 2024TD-06) and Shaanxi Key research & Development Project (No. 2023-ZDLSF-35).

Data availability All relevant raw data, will be freely available to any researcher wishing to use them for non-commercial purposes, without breaching participant confidentiality.

Declarations

Ethics approval and consent to participate All methods were carried out in accordance with the institutional guidelines and regulations. The patient data we used were acquired by publicly available datasets that were collected with patients' informed consent. For the collection of clinical samples, all patients signed the informed consent forms before the specimens were obtained. Our study was approved by the Human Subjects Committee of Xijing Hospital, Xi'an, China.

Competing interests The authors declare that they have no competing interests.

Animal ethics Not applicable.

Open Access This article is licensed under a Creative Commons Attribution-NonCommercial-NoDerivatives 4.0 International License, which permits any non-commercial use, sharing, distribution and reproduction in any medium or format, as long as you give appropriate credit to the original author(s) and the source, provide a link to the Creative Commons licence, and indicate if you modified the licensed material. You do not have permission under this licence to share adapted material derived from this article or parts of it. The images or other third party material in this article are included in the article's Creative Commons licence, unless indicated otherwise in a credit line to the material. If material is not included in the article's Creative Commons licence and your intended use is not permitted by statutory regulation or exceeds the permitted use, you will need to obtain permission directly from the copyright holder. To view a copy of this licence, visit <http://creativecommons.org/licenses/by-nc-nd/4.0/>.

References

1. Sung H, Ferlay J, Siegel RL, Laversanne M, Soerjomataram I, Jemal A, Bray F. Global Cancer statistics 2020: GLOBOCAN estimates of incidence and Mortality Worldwide for 36 cancers in 185 countries. *CA Cancer J Clin.* 2021;71:209–49.
2. Ajani JA, D'Amico TA, Brentner DJ, Chao J, Cooke D, Corvera C, Das P, Enzinger PC, Enzler T, Fanta P, Farjah F, Gerdes H, Gibson MK, Hochwald S, Hofstetter WL, Ilson DH, Keswani RN, Kim S, Kleinberg LR, Klempner SJ, Lacy J, Ly QP, Matkowskyj KA, McNamara M, Mulcahy MF, Outlaw D, Park H, Perry KA, Pimiento J, Poultsides GA, Reznik S, Roses RE, Strong VE, Su S, Wang HL, Wiesner G, Willett CG, Yakoub D, Yoon H, McMillian N, Pluchino LA. Gastric cancer, version 2.2022, NCCN clinical practice guidelines in oncology. *J Natl Compr Canc Netw.* 2022;20:167–92.
3. Smyth EC, Nilsson M, Grabsch HI, van Grieken NC, Lordick F. Gastric cancer. *Lancet.* 2020;396:635–48.
4. Kumar V, Ramnarayanan K, Sundar R, Padmanabhan N, Srivastava S, Koiwa M, Yasuda T, Koh V, Huang KK, Tay ST, Ho SWT, Tan ALK, Ishimoto T, Kim G, Shabbir A, Chen Q, Zhang B, Xu S, Lam K-P, Lum HYJ, Teh M, Yong WP, So JBY, Tan P. Single-cell atlas of Lineage States, Tumor Microenvironment, and subtype-specific expression programs in gastric Cancer. *Cancer Discov.* 2022;12:670–91.
5. Zeng D, Wu J, Luo H, Li Y, Xiao J, Peng J, Ye Z, Zhou R, Yu Y, Wang G, Huang N, Wu J, Rong X, Sun L, Sun H, Qiu W, Xue Y, Bin J, Liao Y, Li N, Shi M, Kim K-M, Liao W. Tumor microenvironment evaluation promotes precise checkpoint immunotherapy of advanced gastric cancer. *J Immunother Cancer.* 2021;9(8):e002467.
6. Rihawi K, Ricci AD, Rizzo A, Brocchi S, Marasco G, Pastore LV, Llimpe FLR, Golfieri R, Renzulli M. Tumor-associated macrophages and inflammatory microenvironment in gastric cancer: novel translational implications. *Int J Mol Sci.* 2021;22(8):3805.
7. Gambardella V, Castillo J, Tarazona N, Gimeno-Valiente F, Martínez-Ciarpaglini C, Cabeza-Segura M, Roselló S, Roda D, Huerta M, Cervantes A, Fleitas T. The role of tumor-associated macrophages in gastric cancer development and their potential as a therapeutic target. *Cancer Treat Rev.* 2020;86:102015.
8. Huang W, Jiang Y, Xiong W, Sun Z, Chen C, Yuan Q, Zhou K, Han Z, Feng H, Chen H, Liang X, Yu S, Hu Y, Yu J, Chen Y, Zhao L, Liu H, Zhou Z, Wang W, Wang W, Xu Y, Li G. Noninvasive imaging of the tumor immune microenvironment correlates with response to immunotherapy in gastric cancer. *Nat Commun.* 2022;13:5095.
9. Yamaguchi T, Fushida S, Yamamoto Y, Tsukada T, Kinoshita J, Oyama K, Miyashita T, Tajima H, Ninomiya I, Munesue S, Harashima A, Harada S, Yamamoto H, Ohta T. Tumor-associated macrophages of the M2 phenotype contribute to progression in gastric cancer with peritoneal dissemination. *Gastric Cancer Off J Int Gastric Cancer Assoc Japanese Gastric Cancer Assoc.* 2016;19:1052–65.
10. Tiainen S, Tumelius R, Rilla K, Hämäläinen K, Tammi M, Tammi R, Kosma V-M, Oikari S, Auvinen P. High numbers of macrophages, especially M2-like (CD163-positive), correlate with hyaluronan accumulation and poor outcome in breast cancer. *Histopathology.* 2015;66:873–83.
11. Goldman MJ, Craft B, Hastie M, Repčeka K, McDade F, Kamath A, Banerjee A, Luo Y, Rogers D, Brooks AN, Zhu J, Haussler D. Visualizing and interpreting cancer genomics data via the Xena platform. *Nat Biotechnol.* 2020;38:675–8.
12. Newman AM, Steen CB, Liu CL, Gentles AJ, Chaudhuri AA, Scherer F, Khodadoust MS, Esfahani MS, Luca BA, Steiner D, Diehn M, Alizadeh AA. Determining cell type abundance and expression from bulk tissues with digital cytometry. *Nat Biotechnol.* 2019;37:773–82.
13. Langfelder P, Horvath S. WGCNA: an R package for weighted correlation network analysis. *BMC Bioinformatics.* 2008;9:559.
14. Subramanian A, Tamayo P, Mootha VK, Mukherjee S, Ebert BL, Gillette MA, Paulovich A, Pomeroy SL, Golub TR, Lander ES, Mesirov JP. Gene set enrichment analysis: a knowledge-based approach for interpreting genome-wide expression profiles. *Proc Natl Acad Sci U S A.* 2005;102:15545–50.
15. Rizzo A, Ricci AD, Brandi G. PD-L1, TMB, MSI, and other predictors of response to Immune checkpoint inhibitors in biliary Tract Cancer. *Cancers (Basel).* 2021;13(3):558.
16. Mayakonda A, Lin D-C, Assenov Y, Plass C, Koeffler HP. Maftools: efficient and comprehensive analysis of somatic variants in cancer. *Genome Res.* 2018;28:1747–56.
17. Newman AM, Liu CL, Green MR, Gentles AJ, Feng W, Xu Y, Hoang CD, Diehn M, Alizadeh AA. Robust enumeration of cell subsets from tissue expression profiles. *Nat Methods.* 2015;12:453–7.
18. Fu J, Li K, Zhang W, Wan C, Zhang J, Jiang P, Liu XS. Large-scale public data reuse to model immunotherapy response and resistance. *Genome Med.* 2020;12:21.
19. Shankavaram UT, Varma S, Kane D, Sunshine M, Chary KK, Reinhold WC, Pommier Y, Weinstein JN. CellMiner: a relational database and query tool for the NCI-60 cancer cell lines. *BMC Genomics.* 2009;10:277.
20. Geeleher P, Cox N, Huang RS. pRRophetic: an R package for prediction of clinical chemotherapeutic response from tumor gene expression levels. *PLoS ONE.* 2014;9:e107468.
21. Samstein RM, Lee C-H, Shoushtari AN, Hellmann MD, Shen R, Janjigian YY, Barron DA, Zehir A, Jordan EJ, Omuro A, Kaley TJ, Kendall SM, Motzer RJ, Hakimi AA, Voss MH, Russo P, Rosenberg J, Iyer G, Bochner BH, Bajorin DF, Al-Ahmadie HA, Chaft JE, Rudin CM, Riely GJ, Baxi S, Ho AL, Wong RJ, Pfister DG, Wolchok JD, Barker CA, Gutin PH, Brennan CW, Tabar V, Mellingerhoff IK, DeAngelis LM, Ariyan CE, Lee N, Tap WD, Gounder MM, D'Angelo SP, Saltz L, Stadler ZK, Scher HI, Baselga J, Razavi P, Klebanoff CA, Yaeger R, Segal NH, Ku GY, DeMatteo RP, Ladanyi M, Rizvi NA, Berger MF, Riaz N, Solit DB, Chan TA, Morris LGT. Tumor mutational load predicts survival after immunotherapy across multiple cancer types. *Nat Genet.* 2019;51:202–6.
22. Ke L, Li S, Huang D. The predictive value of tumor mutation burden on survival of gastric cancer patients treated with immune checkpoint inhibitors: a systematic review and meta-analysis. *Int Immunopharmacol.* 2023;124:110986.
23. Cao D, Xu H, Xu X, Guo T, Ge W. High tumor mutation burden predicts better efficacy of immunotherapy: a pooled analysis of 103078 cancer patients. *Oncoimmunology.* 2019;8:e1629258.
24. Cheong J-H, Wang SC, Park S, Porembka MR, Christie AL, Kim H, Kim HS, Zhu H, Hyung WJ, Noh SH, Hu B, Hong C, Karalis JD, Kim I-H, Lee SH, Hwang TH. Development and validation of a prognostic and predictive 32-gene signature for gastric cancer. *Nat Commun.* 2022;13:774.
25. Cho JY, Lim JY, Cheong JH, Park Y-Y, Yoon S-L, Kim SM, Kim S-B, Kim H, Hong SW, Park YN, Noh SH, Park ES, Chu I-S, Hong WK, Ajani JA, Lee J-S. Gene expression signature-based prognostic risk score in gastric cancer. *Clin Cancer Res.* 2011;17:1850–7.

26. Chen D, Fu M, Chi L, Lin L, Cheng J, Xue W, Long C, Jiang W, Dong X, Sui J, Lin D, Lu J, Zhuo S, Liu S, Li G, Chen G, Yan J. Prognostic and predictive value of a pathomics signature in gastric cancer. *Nat Commun.* 2022;13:6903.
27. Zeng D, Li M, Zhou R, Zhang J, Sun H, Shi M, Bin J, Liao Y, Rao J, Liao W. Tumor Microenvironment characterization in gastric Cancer identifies prognostic and immunotherapeutically relevant Gene signatures. *Cancer Immunol Res.* 2019;7:737–50.
28. Cao Y, Qiao B, Chen Q, Xie Z, Dou X, Xu L, Ran H, Zhang L, Wang Z. Tumor microenvironment remodeling via targeted depletion of M2-like tumor-associated macrophages for cancer immunotherapy. *Acta Biomater.* 2023;160:239–51.
29. Ito A, Kagawa S, Sakamoto S, Kuwada K, Kajioka H, Yoshimoto M, Kikuchi S, Kuroda S, Yoshida R, Tazawa H, Fujiwara T. Extracellular vesicles shed from gastric cancer mediate protumor macrophage differentiation. *BMC Cancer.* 2021;21:102.
30. Luo Q, Zheng N, Jiang L, Wang T, Zhang P, Liu Y, Zheng P, Wang W, Xie G, Chen L, Li D, Dong P, Yuan X, Shen L. Lipid accumulation in macrophages confers protumorigenic polarization and immunity in gastric cancer. *Cancer Sci.* 2020;111:4000–11.
31. Yin S, Huang J, Li Z, Zhang J, Luo J, Lu C, Xu H, Xu H. The prognostic and clinicopathological significance of tumor-associated macrophages in patients with gastric cancer: a meta-analysis. *PLoS ONE.* 2017;12:e0170042.
32. Shah MA, Enzinger P, Ko AH, Ocean AJ, Philip PA, Thakkar PV, Cleveland K, Lu Y, Kortmansky J, Christos PJ, Zhang C, Kaur N, Elmonshed D, Galletti G, Sarkar S, Bhinder B, Pittman ME, Plotnikova OM, Kotlov N, Frenkel F, Bagaev A, Elemento O, Betel D, Giannakakou P, Lenz H-J. Multicenter Phase II study of cabazitaxel in advanced gastroesophageal cancer: association of HER2 expression and M2-like tumor-associated macrophages with patient outcome. *Clin Cancer Res.* 2020;26:4756–66.
33. Zheng P, Luo Q, Wang W, Li J, Wang T, Wang P, Chen L, Zhang P, Chen H, Liu Y, Dong P, Xie G, Ma Y, Jiang L, Yuan X, Shen L. Tumor-associated macrophages-derived exosomes promote the migration of gastric cancer cells by transfer of functional Apolipoprotein E. *Cell Death Dis.* 2018;9:434.
34. Chen S, Li Y, Zhu Y, Fei J, Song L, Sun G, Guo L, Li X. SERPINE1 overexpression promotes malignant progression and poor prognosis of gastric Cancer. *J Oncol.* 2022;2022:2647825.
35. Wu P-L, He Y-F, Yao H-H, Hu B. Martrilin-3 (MATN3) overexpression in gastric adenocarcinoma and its prognostic significance. *Med Sci Monit.* 2018;24:348–55.
36. Pan J, Fan Z, Wang Z, Dai Q, Xiang Z, Yuan F, Yan M, Zhu Z, Liu B, Li C. CD36 mediates palmitate acid-induced metastasis of gastric cancer via AKT/GSK-3 β / β -catenin pathway. *J Exp Clin Cancer Res.* 2019;38:52.
37. Gu Y, Li T, Kapoor A, Major P, Tang D. Contactin 1: an important and emerging oncogenic protein promoting Cancer Progression and Metastasis. *Genes (Basel).* 2020;11(8):874.
38. Chen D-H, Yu J-W, Wu J-G, Wang S-L, Jiang B-J. Significances of contactin-1 expression in human gastric cancer and knockdown of contactin-1 expression inhibits invasion and metastasis of MKN45 gastric cancer cells. *J Cancer Res Clin Oncol.* 2015;141:2109–20.
39. Addeo A, Friedlaender A, Banna GL, Weiss GJ. TMB or not TMB as a biomarker: that is the question. *Crit Rev Oncol Hematol.* 2021;163:103374.
40. Cheng Y, Bu D, Zhang Q, Sun R, Lyle S, Zhao G, Dong L, Li H, Zhao Y, Yu J, Hao X. Genomic and transcriptomic profiling indicates the prognosis significance of mutational signature for TMB-high subtype in Chinese patients with gastric cancer. *J Adv Res.* 2022;51:121–34.
41. van den Bulk J, Verdegaal EM, de Miranda NF. Cancer immunotherapy: broadening the scope of targetable tumours. *Open Biol.* 2018;8(6):180037.
42. Sivori S, Pende D, Quatrini L, Pietra G, Della Chiesa M, Vacca P, Tumino N, Moretta F, Mingari MC, Locatelli F, Moretta L. NK cells and ILCs in tumor immunotherapy. *Mol Aspects Med.* 2021;80:100870.
43. Mimura K, Kamiya T, Shiraiishi K, Kua L-F, Shabbir A, So J, Yong W-P, Suzuki Y, Yoshimoto Y, Nakano T, Fujii H, Campana D, Kono K. Therapeutic potential of highly cytotoxic natural killer cells for gastric cancer. *Int J Cancer.* 2014;135:1390–8.
44. Liu X, Xu D, Huang C, Guo Y, Wang S, Zhu C, Xu J, Zhang Z, Shen Y, Zhao W, Zhao G. Regulatory T cells and M2 macrophages present diverse prognostic value in gastric cancer patients with different clinicopathologic characteristics and chemotherapy strategies. *J Transl Med.* 2019;17:192.
45. Yang C, Dou R, Wei C, Liu K, Shi D, Zhang C, Liu Q, Wang S, Xiong B. Tumor-derived exosomal microRNA-106b-5p activates EMT-cancer cell and M2-subtype TAM interaction to facilitate CRC metastasis. *Mol Ther.* 2021;29:2088–107.
46. Liu Q, Yang C, Wang S, Shi D, Wei C, Song J, Lin X, Dou R, Bai J, Xiang Z, Huang S, Liu K, Xiong B. Wnt5a-induced M2 polarization of tumor-associated macrophages via IL-10 promotes colorectal cancer progression. *Cell Commun Signal.* 2020;18:51.
47. Lin X, Wang S, Sun M, Zhang C, Wei C, Yang C, Dou R, Liu Q, Xiong B. miR-195-5p/NOTCH2-mediated EMT modulates IL-4 secretion in colorectal cancer to affect M2-like TAM polarization. *J Hematol Oncol.* 2019;12:20.
48. Oh D-Y, Lee K-W, Cho JY, Kang WK, Im S-A, Kim JW, Bang Y-J. Phase II trial of dacomitinib in patients with HER2-positive gastric cancer. *Gastric Cancer Off J Int Gastric Cancer Assoc Japan Gastric Cancer Assoc.* 2016;19:1095–103.
49. Nam H-J, Ching KA, Kan J, Kim H-P, Han S-W, Im S-A, Kim T-Y, Christensen JG, Oh D-Y, Bang Y-J. Evaluation of the antitumor effects and mechanisms of PF00299804, a pan-HER inhibitor, alone or in combination with chemotherapy or targeted agents in gastric cancer. *Mol Cancer Ther.* 2012;11:439–51.
50. Hong JY, Kim HJ, Kim K, Hong J, Kim JE, Byeon S-J, Lee I-K, Kim K-M, Shim M, Park SH, Park JO, Park YS, Lim HY, Kim ST, Lee J, Kang WK. TPK1 as a predictive marker for the anti-tumour effects of simvastatin in gastric cancer. *Pathol Res Pract.* 2020;216:152820.
51. Duarte JA, de Barros ALB, Leite EA. The potential use of simvastatin for cancer treatment: a review. *Biomed Pharmacother.* 2021;141:111858.
52. Xia Y, Jin Y, Cui D, Wu X, Song C, Jin W, Huang H. Antitumor effect of simvastatin in combination with dna methyltransferase inhibitor on gastric cancer via GSDME-mediated pyroptosis. *Front Pharmacol.* 2022;13:860546.